Communication

Formation and Oxidation State of CeO Nanotubes

Wei-Qiang Han, Lijun Wu, and Yimei Zhu

J. Am. Chem. Soc., **2005**, 127 (37), 12814-12815• DOI: 10.1021/ja054533p • Publication Date (Web): 23 August 2005

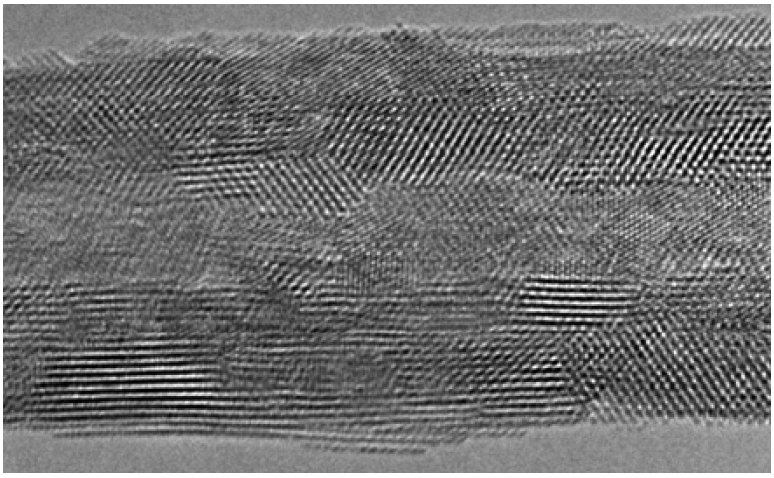

J|A|C|S
COMMUNICATIONS

Published on Web 08/23/2005

Formation and Oxidation State of CeO_{2-x} Nanotubes

Wei-Qiang Han,* Lijun Wu, and Yimei Zhu

Center for Functional Nanomaterials, Brookhaven National Laboratory, Upton, New York 11973-5000

Received July 8, 2005; E-mail: whan@bnl.gov

In recent years, many synthesis efforts have been placed on the ceria (i.e., CeO_{2-x}) nanoparticles.[1] Ceria nanoparticles are used not only as excellent automobile exhaust catalysts but also in high-energy efficiency fuel-cells, polishing materials, additives in ceramics, and phosphors.[2,3] Very recently, ceria nanowires have been reported through several synthesis routes, including a sol−gel process within the nanochannels of porous anodic alumina templates, nonisothermal precipitation, spontaneous self-assembly of cerium oxide nanoparticles to nanorods, and a solution-based hydrothermal method by using an autoclave.[4,5]

Oxide nanotubes, needled-shaped oxide crystals with hollow channels along the needle axis, such as SiO_2, TiO_2, EuO, Y_2O_3, $BaTiO_3$, $PbTiO_3$, Co_3O_4, $H_2Ti_3O_7$, and VO_x, are of interest because they might offer novel properties and lead directly to new technological applications.[6] They are usually made by using templates, or a high-temperature reaction or a hydrothermal process with high pressure. Yang et al. reported the formation of fluorite CeO_2 nanotubes and $Ce(OH)CO_3$ by a hydrothermal method using $Ce^{4+}(NO_3)_4$ as the Ce source, octadecylamine as the surfactant template, and urea as a precipitation agent.[7]

Here, we report a hydrothermal route with mild reaction conditions (without using high pressure and high temperature). We study the shapes, structure, and oxide state properties by X-ray diffraction (XRD), high-resolution transmission electron microscopy (HRTEM), and electron energy-loss spectroscopy (EELS).

The CeO_{2-x} nanotubes were synthesized by two successive stages: precipitation and aging. At the precipitation stage, 0.9 g of cerium nitrate ($Ce(NO_3)_3 \cdot 6H_2O$) was added to 10 mL of deionized water and heated at 100 °C. Once a large amount of vapor formed, 7 mL of 5% ammonia hydroxide solution was added. Very fine yellowish precipitates were formed immediately and started to boil. After 3 min, the solution was quickly transferred and cooled at 0 °C. After 45 days aging, we took a sample out for XRD and TEM measurements. The XRD pattern of the sample was recorded by a Rigaku/Miniflex spectrometer with Cu Kα irradiation. We dispersed the solution on TEM copper grids that were covered with lacy carbon. The sample was then examined in a field emission TEM operated at 300 kV.

Figure 1a shows an XRD spectrum of the sample aged for 45 days. The characteristic peaks shown in the spectrum reveal that the powders have a cubic fluorite structure which is the same as that of bulk CeO_2. However, the lattice parameter measured by XRD is 0.54231 nm, which is larger than that of the bulk CeO_2 crystal (JCPDS# 43-1002, $a = 0.541134$ nm). Figure 1b is a selected-area electron diffraction pattern containing a few CeO_{2-x} nanotubes, conforming that the CeO_{2-x} nanotubes are cubic fluorite structure, as well.

Figure 2a shows a low-magnification TEM image of the sample. In addition to a small fraction of CeO_{2-x} nanoparticles, most powders are one-dimensional nanostructures of CeO_{2-x}. A careful inspection reveals that there are two kinds of one-dimensional nanostructures of CeO_{2-x}. One is the nanowire with consistent lattice

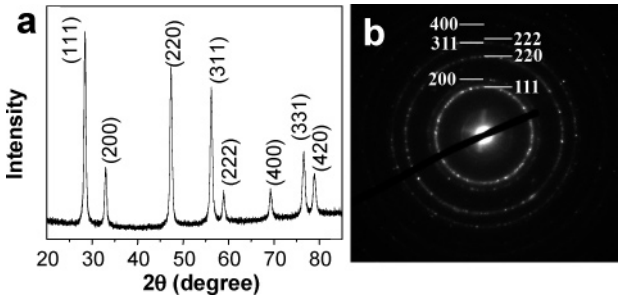

Figure 1. (a) X-ray diffraction of the sample aged for 45 days. All peaks can be indexed by face-centered cubic with $a = 0.54231$ nm. (b) Selected-area electron diffraction pattern with a few CeO_{2-x} nanotubes; all rings are indexed as a fcc lattice.

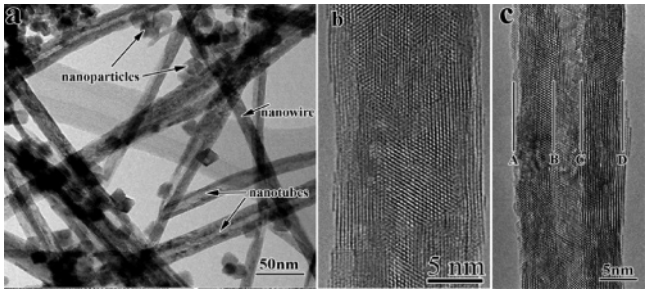

Figure 2. (a) Typical morphology of the sample. There are three kinds of nanostructures: nanoparticles, nanowires, and nanotubes as marked in the figure. (b) High-resolution image of a nanowire. (c) High-resolution image of a nanotube. The thickness of the wall of the nanotube is about 5.5 nm by measuring the spacing between lines A and B or lines C and D.

across, while the other is the nanotube with weak contrast in the middle. These characteristics can be seen more clearly in the high-resolution images shown in Figure 2b,c. Both CeO_{2-x} nanowires and nanotubes are crystalline and tend to align their (111) plane parallel to the axis direction. The diameter of the nanowires and nanotubes ranges from 5 to 30 nm, while the length is up to several microns. For most nanotubes, the thickness of the wall is quite uniform over the tube, though they change from tube to tube. The shapes of the nanotubes do not change significantly when the nanotubes are tilted along their axis directions, indicating that they have cylinder geometry. On the basis of the analysis of electron diffraction and high-resolution imaging, we found that the CeO_{2-x} nanoparticles, nanowires, and nanotubes have the same crystal structure, cubic fluorite structure, which is consistent with the X-ray measurement. The lattice parameter of the CeO_{2-x} nanotubes varies from 0.54 to 0.56 nm, depending on their diameters. In general, the lattice parameter increases with decreasing diameter of the nanotubes.

The increase of the lattice parameter of the CeO_{2-x} nanotubes implies that the oxidation state of the CeO_{2-x} nanotubes may be different from that in bulk CeO_2. It is well-known that the relative intensity of the white lines (M_4 and M_5) of the cerium in the EELS can be used to determine the valence of the cerium ions.[3] Figure 3

10.1021/ja054533p CCC: $30.25

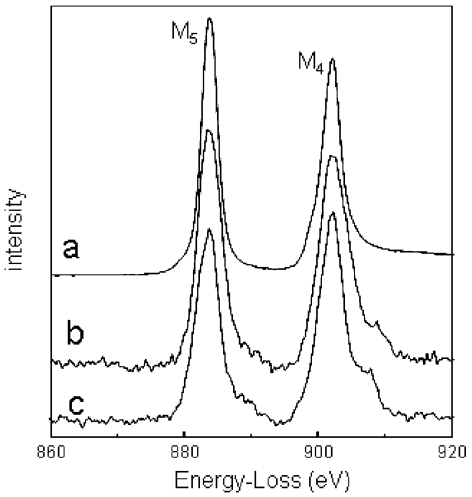

Figure 3. EELS spectra showing different M_5 peak intensity for CeO_{2-x} nanotubes with (a) $d = 14.6$ nm, (b) $d = 17.3$ nm, and (c) $d = 25.5$ nm. The thicknesses of the wall of the nanotubes are 5.5, 6.0, and 10.8 nm for a, b, and c, respectively. The spectra are normalized for the M_4 peak.

shows M_4 and M_5 edges of the EELS spectra from three nanotubes with diameter $d = 14.6$, 17.3, and 25.5 nm, respectively. It qualitatively illustrates a systematic change in the EELS spectra with the diameters of the nanotubes; for example, the intensity of the M_5 edge increases with the decrease of the diameter of the nanotubes. To determine the relative amounts of cerium ions, Ce^{3+} and Ce^{4+}, we use the second derivative method to measure the M_5/M_4 ratio since it is insensitive to thickness variations (for details, see ref 3). The M_5/M_4 ratio for $d = 14.6$, 17.3, and 25.5 nm is measured to be 1.27, 1.22, and 1.05, respectively. Based on M_5/M_4 being 1.31 for Ce^{3+} and 0.91 for Ce^{4+}, the fraction of Ce^{3+} ($Ce^{3+}/[Ce^{3+} + Ce^{4+}]$) is, therefore, estimated to be 0.90, 0.78, and 0.35 for $d = 14.6$, 17.3, and 25.5 nm, respectively. Compared to the CeO_{2-x} nanoparticles,[3] the fraction of Ce^{3+} in the CeO_{2-x} nanotubes is significantly larger than that of CeO_{2-x} nanoparticles with the same diameter. The main reason is that, for nanotubes, there are two surfaces: the outer surface and the inner surface. Actually, the total surface area depends on the thickness of the wall of the nanotubes. If the cerium ions in the CeO_{2-x} nanotubes follow the same distribution of the CeO_{2-x} nanoparticles, that is, Ce^{3+} exists on the surface, while Ce^{4+} inside,[3] the fraction of Ce^{3+} would mainly depend on the thickness of the wall. In fact, the thicknesses of the wall of the nanotubes for Figure 3a−c are about 5.5, 6.0, and 10.8 nm, respectively.

Zhou et al. added an aqueous ammonium hydroxide precipitant into cerium nitrate solution at room temperature and introduced oxygen into the reactor to oxidized Ce^{3+} to Ce^{4+}. They only obtained CeO_2 nanoparticles.[8] Chen et al. added an aqueous ammonium hydroxide precipitant into cerium nitrate at 70 °C and subsequently aged at 0 °C for 1 day. They only got CeO_{2-x} nanowires.[5] In our experiment, we added an aqueous ammonium hydroxide to cerium nitrate solution, but the precipitation temperature was used at 100 °C and subsequently aged at 0 °C. When the sample was taken out after aging for 1 day, we found many nanowires and some nanotubes. This means that higher precipitation temperature is key for the formation of the tubular structures. As we reported above, a large amount of nanotubes were formed in the sample after aging for 45 days. This shows that long-time aging plays another important role for the formation of tubular structure. Cerium nitrate solution reacts with ammonium hydroxide to form $Ce(OH)_3$ as mediate product, which has one-dimensional structure and is retained if the pH value of reaction is higher than 8.[9] Excess ammonium hydroxide was used in our experiment, so the mediate Ce^{3+} oxidized to Ce^{4+}. Quickly cooling the samples to 0 °C retained the one-dimensional nanostructure. The precipitates were further dehydrated and recrystallized during the aging time. Longer aging time leads to more one-dimensional structures having hollow structure (i.e., nanotubes).

Cerium oxide has applications as three-way catalysts for its oxygen storage capacity, in diesel fuels for a more complete combustion to abate soot formation, and high-energy efficiency and energy density solid-oxide fuel-cells.[1] The key to these usages depends on its ease of releasing oxygen in a low-oxygen environment, with its characteristic feature to shift between Ce^{4+} and Ce^{3+} in the stable fluorite structure, which, in fact, allows release and transport of O^{2-} ions.[10] Oxygen vacancies in ceria nanotube combined with its inner and outer surface feature could, therefore, offer a more functional and effective manner and play an essential role in applications, such as catalytic reactions.

In summary, we have first reported a simple and easy way to synthesize CeO_{2-x} nanotubes which have a cubic fluorite structure. The measurement of the ratio of the M_5/M_4 edge shows the valence reduction of cerium ions for the CeO_{2-x} nanotubes. The formation of the tubular structure strongly depends on the precipitation temperature and aging time. This mild reaction route could also be useful for synthesis of other nanotubes.

Acknowledgment. This work is supported by the U.S. DOE under Contract DE-AC02-98CH10886.

Supporting Information Available: High-resolution figure of the CeO_{2-x} nanotube. This material is available free of charge via the Internet at http://pubs.acs.org.

References

(1) (a) Zhang, J.; Ju, X.; Wu, Z. Y.; Liu, T.; Hu, T. D.; Xie, Y. N.; Zhang, Z. L. *Chem. Mater*. **2001**, *13*, 4192. (b) Sayle, D. C.; Maicaneanu, S. A.; Watson, G. W. *J. Am. Chem. Soc.* **2002**, *124*, 11429. (c) Shao, Z.; Haile, S. M.; Ahn, J.; Ronney, P. D.; Zhan, Z. L.; Barnett, S. A. *Nature* **2005**, *435*, 795. (d) Trovarelli, A. *Catalysis by Ceria and Related Materials*; Imperial College Press: London, 2002.

(2) (a) Powell, B. R.; Bloink, R. L.; Erckel, C. C. *J. Am. Ceram. Soc.* **1988**, *17*, 104. (b) Kosynkin, V. D.; Arzgatkina, A. A.; Ivanov, E. N.; Chtoutsa, M. G.; Grabko, A. I.; Kardapolov, A. V.; Sysina, N. A. *J. Alloys Compd.* **2000**, *303*−*304*, 421. (c) Messing, G. L.; Zhang, S. C.; Jayanthi, G. V. *J. Am. Ceram. Soc.* **1993**, *76*, 2707. (d) Patsalas, P.; Logothetidis, S.; Metaxa, C. *Appl. Phys. Lett.* **2002**, *81*, 466. (e) Wang, Z. L.; Feng, X. D. *J. Phys. Chem. B* **2003**, *107*, 13563.

(3) Wu, L.; Wiesmann, H. J.; Moodenbaugh, A. R.; Klie, R. F.; Zhu, Y.; Welch, D. O.; Suenaga, M. *Phys. Rev.* **2004**, *B69*, 125415.

(4) (a) Wu, G.; Xie, T.; Yuan, X.; Cheng, B.; Zhang, L. *Mater. Res. Bull.* **2004**, *39*, 1023. (b) Kuiry, S.; Patil, S.; Deshpande, S.; Seal, S. *J. Phys. Chem*. *B* **2005**, *109*, 6936. (c) Zhou, K. Wang, X.; Sun, X.; Ping Q.; Li, Y. *J. Catal*. **2005**, *229*, 206.

(5) Chen, H. I.; Chang, H. Y. *Solid State Commun*. **2005**, *133*, 593.

(6) (a) Mitchell, D. T.; Lee, S. B.; Trofin, L.; Li, N.; Nevanen, T. K.; Soderlund H.; Martin, C. R. *J. Am. Chem. Soc*. **2002**, *124*, 11864. (b) Fan, R.; Wu, Y.; Li, D.; Yue, M.; Majumdar, A.; Yang, P. *J. Am. Chem. Soc*. **2003**, *125*, 5254. (c) Tian, Z. R.; Voigt, J. A.; Liu, J.; Mckenzie, B.; Xu, H. *J. Am. Chem. Soc*. **2003**, *125*, 12384. (d) Li, D.; Xie, Y. *Nano Lett.* **2004**, *4*, 933. (e) Zhang, S.; Peng, L. M.; Chen, Q.; Du, G. H.; Dawson, G.; Zhou, W. Z. *Phys. Rev. Lett*. **2003**, *91*, 256103. (f) Krusin-Elbaum, L.; Newns, D. M.; Zeng, H.; Derycke, V.; Sun, J. Z.; Sandstrom, R. *Nature* **2004**, *431*, 264. (g) Satishkumar, B.; Govindaraj, A.; Vogl, E.; Basumallick, L.; Rao, C. N. R. *J. Mater. Res.* **1997**, *12*, 604. (h) Krumeich, F.; Muhr, H.; Niederberger, M.; Bieri, F.; Schnyder, B.; Nesper, R. *J. Am. Chem. Soc*. **1999**, *121*, 8324.

(7) Yang, R.; Guo, L. Chin. *J. Inorg. Chem*. **2004**, *20*, 152.

(8) Zhou, X. D.; Huebner, W.; Anderson, H. U. *Appl. Phys. Lett*. **2002**, *80*, 3814.

(9) Yamashita, M.; Kameyama, K.; Yabe, S.; Yoshida, S.; Fujishiro, Y.; Kawai, T.; Sato. T. *J. Mater. Sci*. **2002**, *37*, 683.

(10) (a) Tsunekawa, S.; Ishikawa, K.; Li, Z.; Kawazoe, Y.; Kasuya, A. *Phys. Rev. Lett.* **2000**, *85*, 3440. (b) Trovarelli, A. *Catal. Rev. Sci. Eng.* **1996**, *38*, 439. (c) Rodriguez, J. A.; Jirsak, T.; Freitag, A.; Hanson, J. C.; Larese, J. Z.; Chaturvedi, S. *Catal. Lett.* **1999**, *62*, 113.

JA054533P